

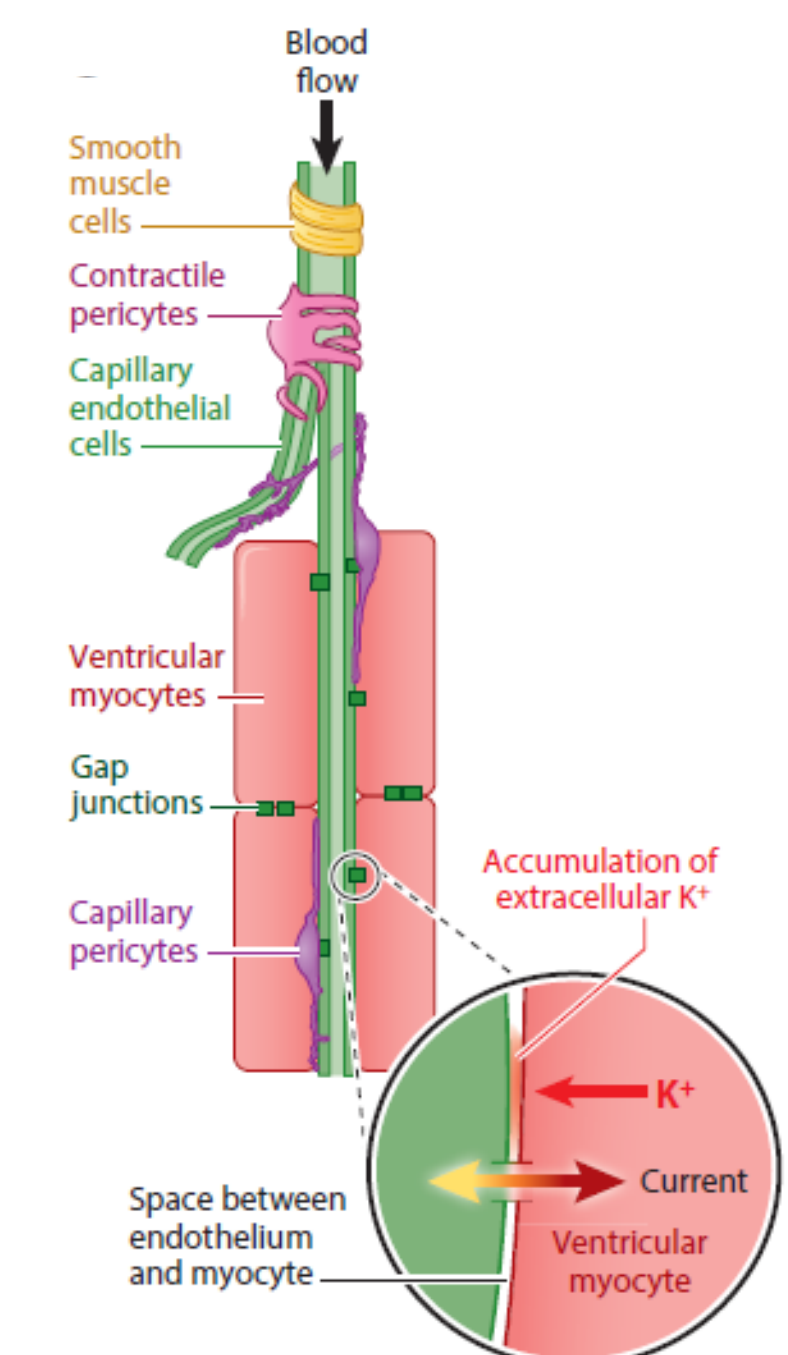
ABSTRACT

Blood flow in the heart is preferentially directed to regions of high metabolic activity while bypassing less active areas with lower demands. This regulation is believed to be highly localized and finely controlled, mediated by a mechanism termed "Electro-Metabolic Signaling" (EMS), identified in both the brain and heart and presumed to exist in other vascular systems. Four key cellular components—ventricular myocytes, capillary endothelial cells, pericytes, and vascular smooth muscle cells—are thought to contribute significantly to EMS in heart. While each element serves several important roles, our study focuses on cardiac pericytes, a type of mural cell that adorns the capillaries in the heart. The dynamic functions and characteristics of the cardiac pericytes under physiological conditions have been difficult to study due to the continuous movement of the beating heart. To address this, we employed a working heart preparation with an intact vascular system at physiological pressures and temperatures (the cardiac Z-Prep, Zhao et al. PNAS 2020). Using a rapid z-stack protocol with a spinning disk confocal microscope, we visualized and quantitatively characterized cardiac pericytes under "physiological" conditions. High-resolution imaging revealed a number of surprising findings. First, pericytes are highly abundant in native cardiac tissue. Second, these cells exhibit extensive spread along capillaries, with significant extensions that traverse the surfaces of adjacent ventricular myocytes and connect to distant capillaries. The pericyte arms often arise from an identified capillary-based pericyte, travel along the surface of one or more ventricular myocytes and terminate on a distant capillary endothelial cell surface. This anatomical organization suggests that pericytes play likely critical roles in signaling, communication, and contractility within the heart. Although pericytes are considered fragile due to their significant loss during isolation procedures, our findings show that they are remarkably robust in their native environment, enduring the dynamic forces of normal cardiac function. These observations underscore the importance of pericytes in normal heart physiology and provide a foundation for future studies on their roles in health and disease.

Acknowledgements. This work is supported by special funds from BioMET.

INTRODUCTION

Understanding cardiac metabolic regulation at high temporal and spatial resolution will contribute fundamentally to the decoding of metabolic syndrome and determine how it is linked to heart diseases. Here we examine the key component of the major new hypothesis in this area which suggests that under normal physiological conditions the metabolic state of local cardiac ventricular myocytes (VMs) themselves regulate their own local blood flow (1, 2). Specifically, the hypothesis posits that ventricular myocytes are able to regulate their own local blood flow by continuously transmitting electrical signals to the capillaries and by that means to the contractile cells of the small vessels. This blood flow regulatory process, called "electro-metabolic signaling," (EMS, Figure 1) indicates that K_{ATP} channels in the ventricular myocytes sense the metabolic state and thereby shape the electrical signal sent through the cECs to pericytes and vascular smooth muscle cells (VSMCs) and consequently regulate blood flow. As one of the key components in EMS, pericytes are thought to play an important role in the regulation of blood flow. However, in heart, high-resolution real-time observations and measurements of pericyte function under physiological conditions are challenging to obtain because of vascular motion, tissue depth and vigorous functional movement. For these reasons, the heart may be one of the most difficult tissues in which to examine pericyte function. Recently, we introduced a perfused papillary muscle preparation (the Z-Prep) that allows us to observe coronary arteries, arterioles, venules, capillaries and myocytes in real time at physiological temperature and pressure while also imaging pericytes (1, 2).



Local blood flow control by electro-metabolic signaling (EMS) in heart. Diagram shows local blood flow is controlled or regulated by electrically connected elements that include myocytes, capillaries, pericytes and arterial smooth muscle cells, with myocytes as master controllers. As cardiac myocytes carry out work, ATP is consumed and ADP is produced and elevated. This leads to the opening of K_{ATP} channels in the cardiac myocytes and which drives EMS. K_{ATP} opening produces a time-averaged hyperpolarization of the cardiac action potential (AP) and the accumulation of K^+ in the subspace between myocytes and capillaries. This leads to the hyperpolarization of capillary endothelial cells (cEC) and the other elements including contractile pericytes in the network through gap junctions. On the other hand, the elevation of extracellular K^+ (through K_{ATP} and other K^+ channels opening during repolarization) activates Kir2.1 in the cECs, resulting in cEC hyperpolarization and upstream contractile pericyte and smooth muscle dilation (1-4).

WORKING MODEL

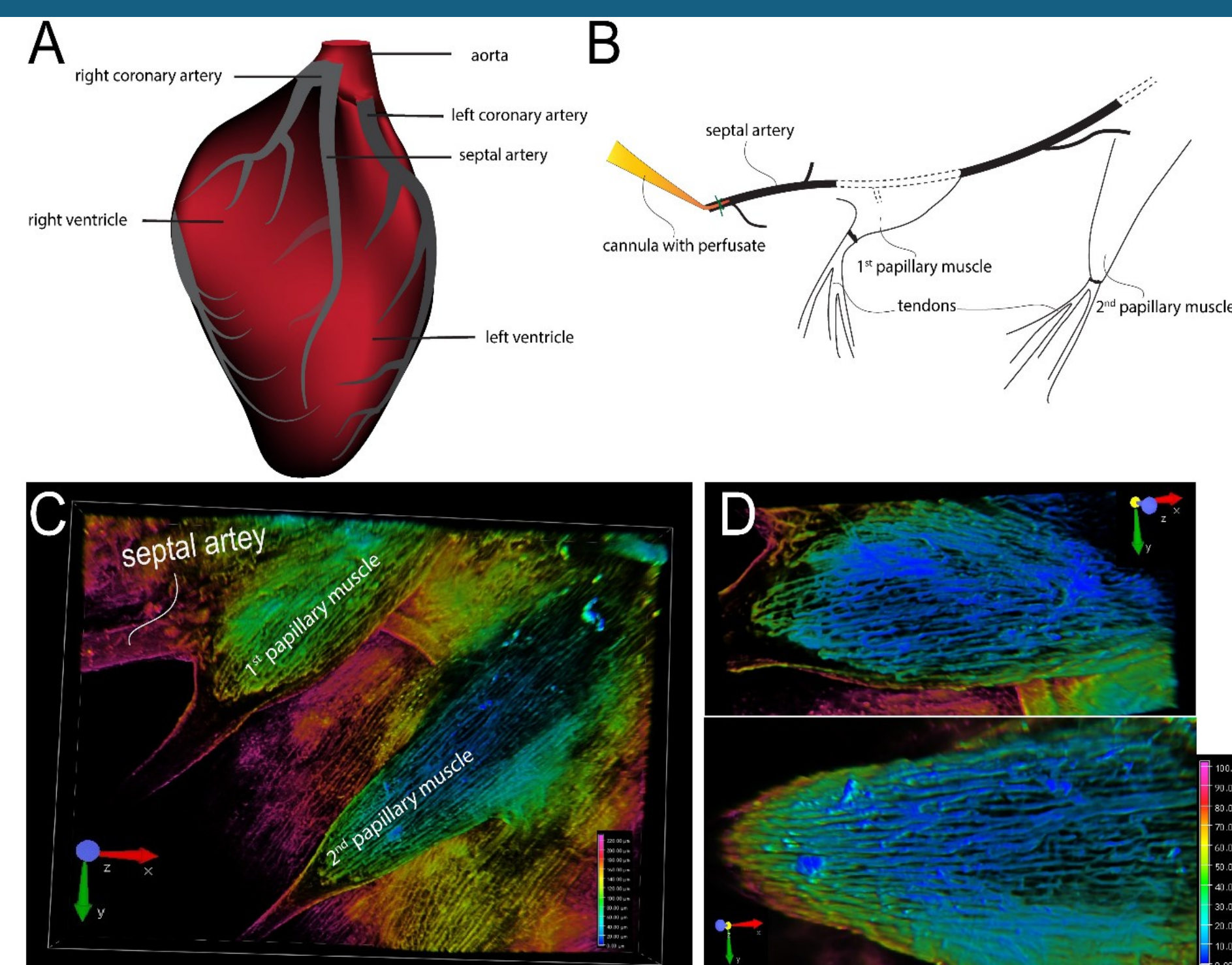


Figure 1. Arterially perfused mouse right ventricle papillary muscle. A. Cartoon shows the origin and course of coronary arteries. Note: septal artery originates from right coronary artery. B. Diagram shows the location of cannula and the papillary muscles. C. Depth-encoded vascular imaging of a Z-prep using WGA-488 as fluorescent marker of the vasculature over a depth of 200 microns. D. Zoomed-in images from C with 1st papillary (top) and 2nd papillary muscle (bottom). Depth encoding over 100 microns.

RESULTS

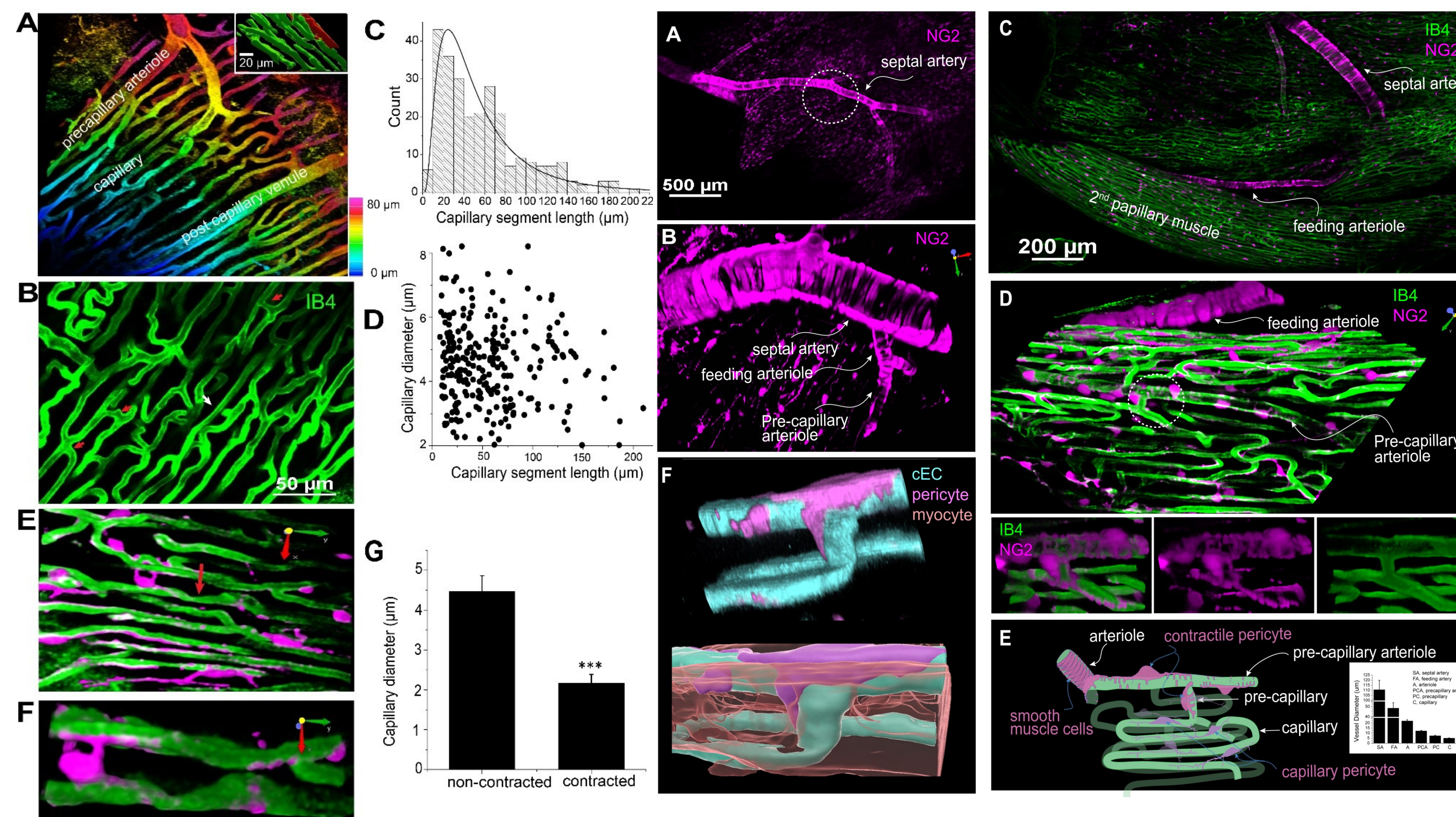


Figure 2. Capillary network geometry and the size in mouse heart (Z-Prep). A. A 3D image with colored depth coding illustrates the organizational hierarchy of precapillary arterioles, the capillary bed, and the postcapillary venule. The inset binary image shows the orientation of capillaries (green) parallel to the myocyte (red). The myocyte was filled with sulforhodamine through microinjection. B. The capillary bed displays varying lengths of capillary segments, with shorter segments indicated by red arrows (< 10 μ m) and longer segments by a white arrow (> 100 μ m). C. A histogram depicts the distribution of different capillary segment lengths. D. A correlation scatterplot of capillary diameter and segment length indicates no significant relationship between the two. E. Examples demonstrate capillary local constriction (arrow) and the location of pericytes (magenta). F. A zoom-in of the arrow-pointed area in E. G. Summary data showing the capillary diameter of non-contracted and local contracted area.

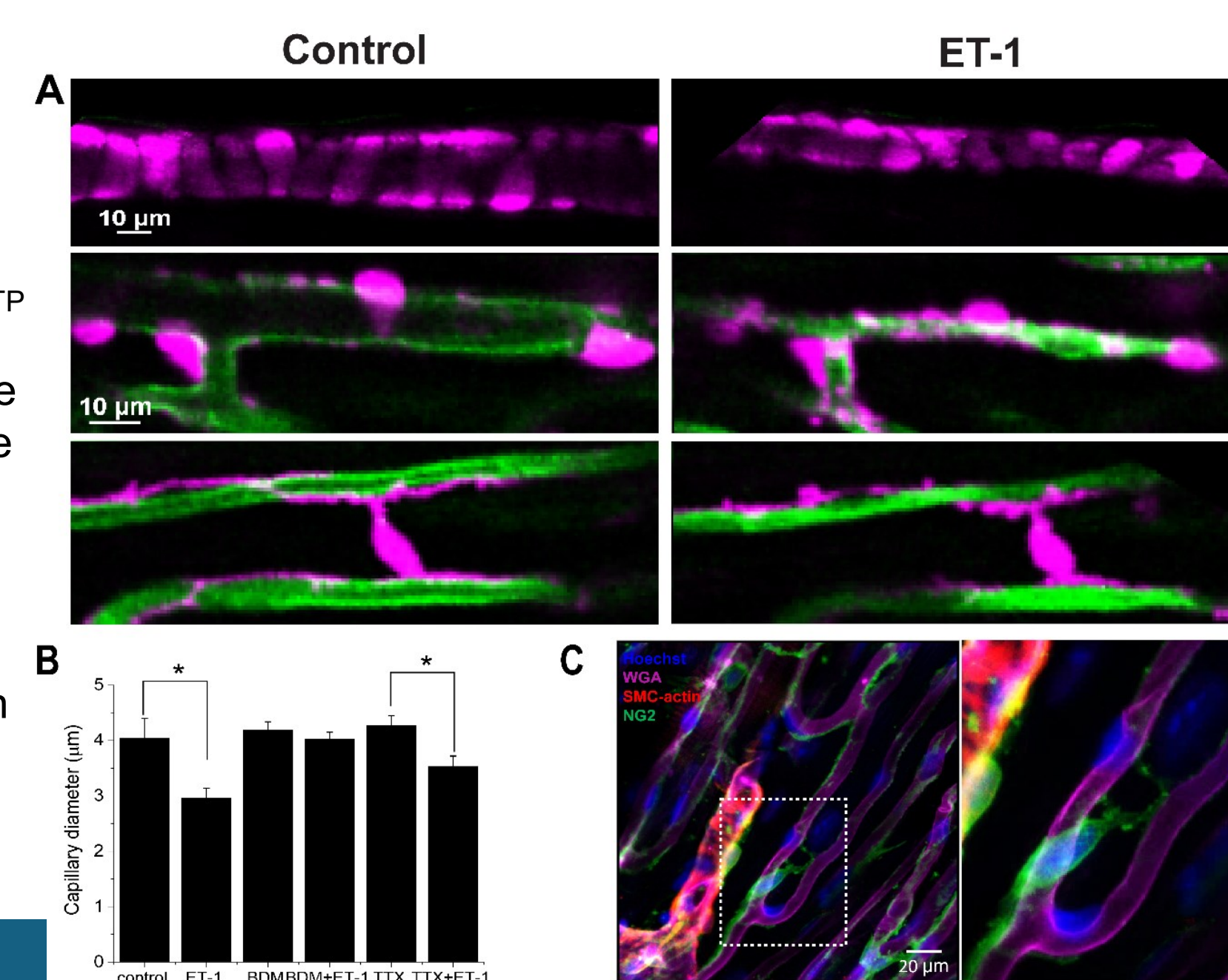


Figure 5. The dynamic change of cardiac pericytes and capillary. A. Images show a feeding arteriole (upper panel), precapillary arteriole (middle) and capillary changes in the presence (left) and absence (right) of ET-1. B. Summary data show capillary diameter change in the presence of ET-1 and/or TTX. * $p < 0.05$. C. Whole-mount immunostaining reveals that smooth muscle actin (SMC-actin, red) is expressed in pre-capillary arteriole smooth muscle cells but not in pericytes (green). The papillary muscle was stained using anti-NG2 (green), anti-SMC-actin (red), WGA (magenta), and Hoechst to identify pericytes, smooth muscle cells, endothelial cells, and nuclei, respectively. Right panel, zoomed-in image of the boxed area in the left panel.

Figure 3. The geometry and structure of the microvascular bed of the mouse right ventricle papillary muscle. A. A representative image of an NG2DsRed mouse heart showing both vascular smooth muscle cells and pericytes that are NG2 positive. B. Zoomed-in region of the circled area in A, showcasing the septal artery, feeding arteriole, and precapillary arteriole through imaging with NG2DsRed. C. A representative image showing the branch of septal artery and feeding arteriole to the 2nd papillary muscle. D. Magnified 3D image of a region of the second papillary muscle showing a high-resolution image of the feeding arteriole, precapillary arterial and capillaries. Lower panel: zoomed-in image of the circled area from main panel. Note that the precapillary arteriole is sparsely covered by the contractile pericytes (often called ensheathing pericytes). E. A cartoon depicting the microvessels and pericytes in papillary microcirculation. Ventricular myocytes fill the "apparently empty" space between the capillaries. F. A pseudo-color 3D rendered image showing a pericyte, capillaries, and a myocyte (lower panel). The myocyte(s) is translucent to show its location with respect to the pericytes and cECs. Note: the angle of the branch is around 90 degrees. A to D are from living Z-Prep in the presence of BDM; F is taken from a fixed heart tissue. The cEC, pericyte, and myocyte are revealed by IB4, NG2 and mitotracker, respectively.

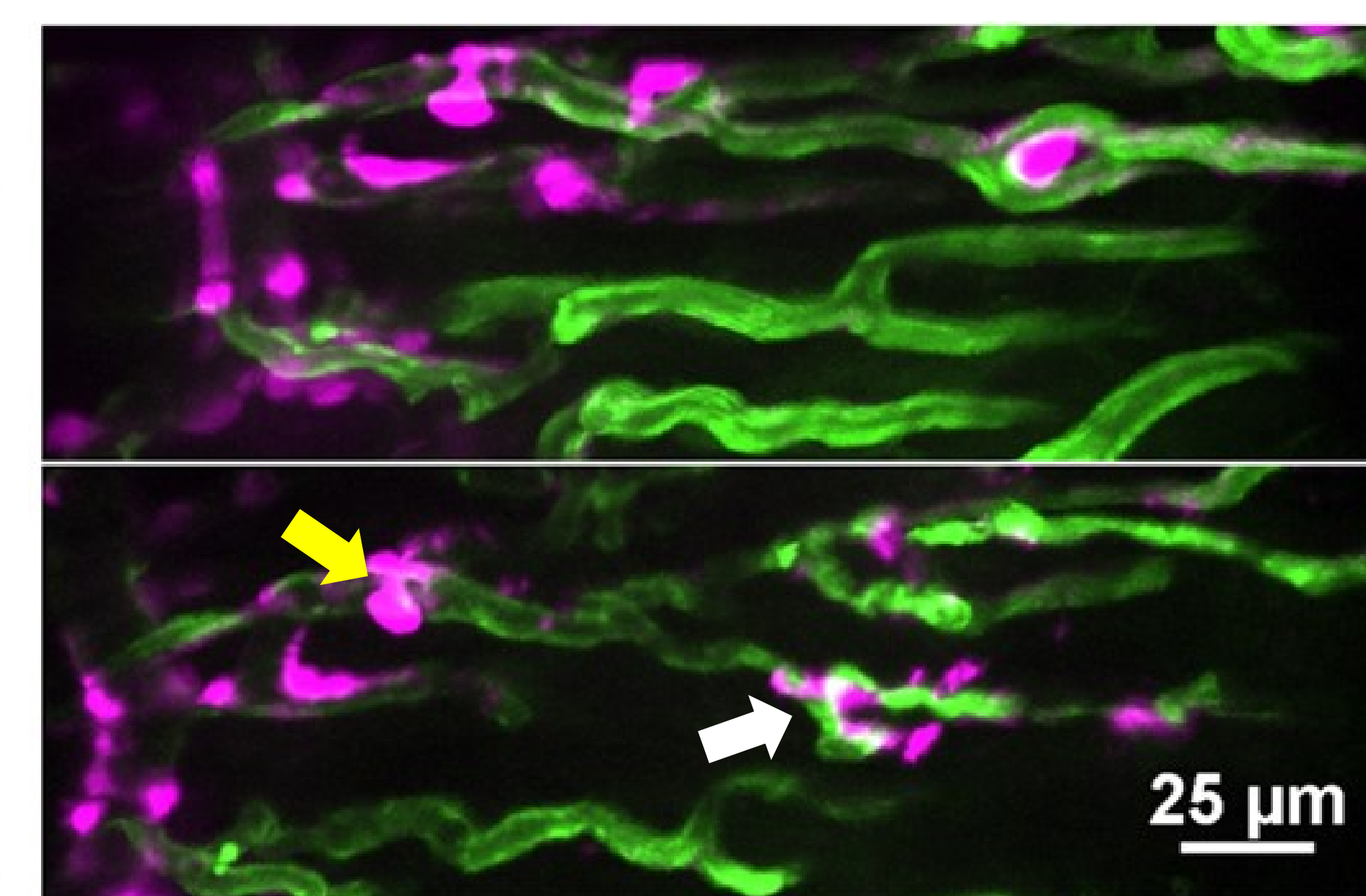


Figure 6. H_2O_2 induces pericyte shedding and irreversible capillary constriction. Images showing the irreversible change of pericyte structure in the presence of H_2O_2 (500 μ M, lower panel). Note the decomposition of capillary pericytes (magenta, white arrow) but not the contractile pericytes (yellow arrow) in the presence of H_2O_2 (lower panel).

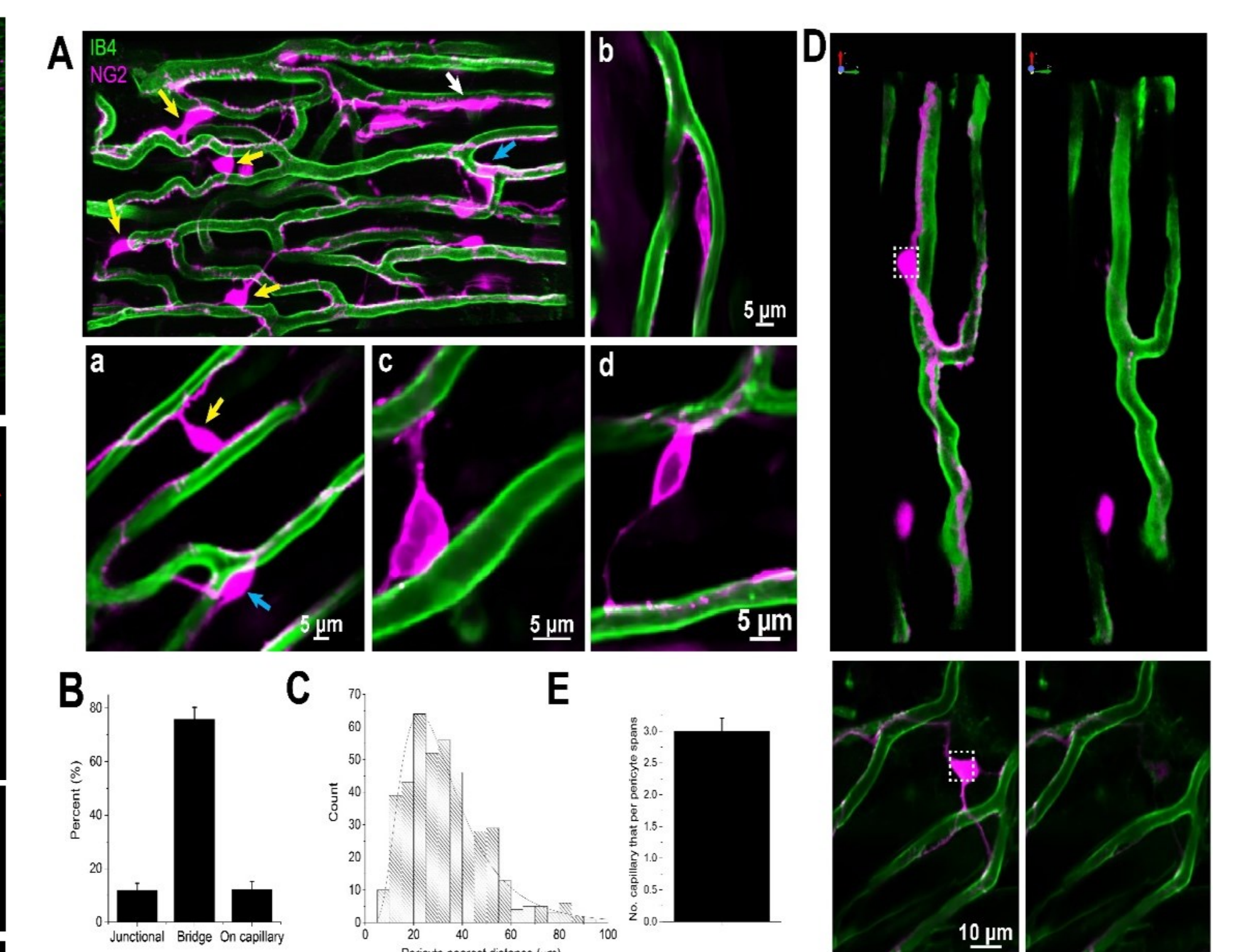


Figure 4. Capillary pericyte geometry and distribution in mouse right ventricle papillary muscle (Z-Prep). A. NG2DsRed mouse heart image displaying pericytes (magenta) and microvessels (green). Various types of pericytes are indicated by arrows: yellow for bridging pericytes located between capillaries, blue for junctional pericytes located at bifurcation area, and white for pericytes located directly on capillaries. Zoomed-in images (Aa to Ad) provide detailed views of pericyte localization. Aa depicts both bridging and junctional pericytes, while Ab shows a pericyte directly attached to a capillary. Ac and Ad highlight bridging pericytes. Pericytes in Ac to Ad are PDGFR β (pink) positive cells. B. Summary data presenting the distribution of different pericyte subtypes. C. Histogram showing the nearest distance between two pericytes. D. Images showing pericytes and their processes before (left panels) and after photo-bleaching (right panels). E. Summary data showing the number of capillaries that each pericyte covers (n=10 pericytes from 2 mouse papillary muscle).

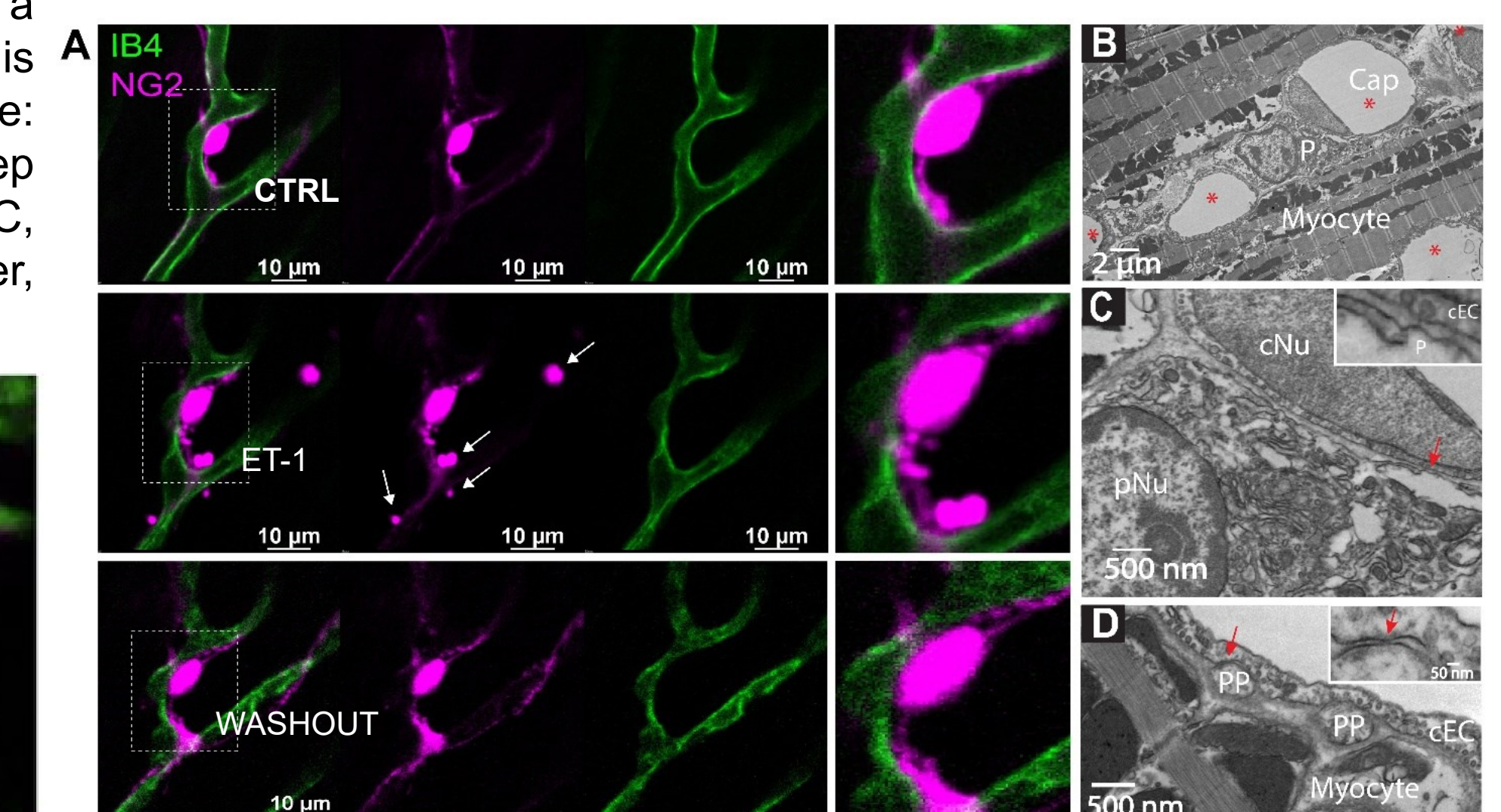


Figure 7. Pericytes Are Not Necessarily Involved in Capillary No-Reflow. A. Images showing the change and restoration of pericyte structure in the presence and absence of ET-1. Note the granulation of pericyte processes (magenta, white arrows) in the presence of ET-1 (middle panel) and the restoration after washing out ET-1 (lower panel), while the capillary lumen remains unaffected. The right panels provide a zoomed-in view of the boxed areas in the left panels. B-D. Transmission Electron Microscopy (TEM) myograph illustrating the structural interaction between pericytes and capillary endothelial cells (cEC) in the mouse heart. B. Cross section of mouse papillary muscle showing five capillaries (Cap, *) and one pericyte soma (P). cNu, capillary endothelial cell nucleus; pNu, pericyte nucleus. Cap, capillary. C. Magnification of the framed area in B. The inset zooms in on the arrowed area in C, showing the distance between the pericyte soma membrane and the cEC membrane. D. Cross section highlighting two pericyte processes (PP). The inset magnifies the junctional structure between the pericyte process membrane and the cEC membrane.

SUMMARY

- Cardiac pericytes, particularly capillary pericytes, exhibit notable heterogeneity, with bridging pericytes showing the greatest variability.
- These cells actively participate in electro-metabolic signaling (EMS), a key regulatory mechanism of cardiac microcirculation.
- Capillary pericytes are dynamically mobile and display heightened susceptibility to reactive oxygen species (ROS).

1. Zhao G, Joca HC, Nelson MT, Lederer WJ. *PNAS* 2020;117(13):7461-70. PMID: PMC7132126.
2. Zhao G, Joca HC, Lederer WJ. *JoVE*. 2020(161). doi: 10.3791/61566.
3. Longden TA, Zhao G, Hariharan A, Lederer WJ. *Ann. Rev. Physiol.* 2023;85:137-64.
4. Longden TA, Lederer WJ. *J. Gen. Physiol.* 2024;156(2). PMID: PMC10783436.

Acknowledgements. This work is supported by special funds from BioMET.